Published by :
http://www.ijert.org

International Journal of Engineering Research & Technology (IJERT)
ISSN: 2278-0181
Vol. 11 Issue 04, April-2022

Improved Relationships for Peak Discharge Estimation at High Return Periods Using Geomorphological Characteristics: Case Study at Sultanate of Oman

Ayman G. Awadallah[1*], Samar A.H. Ali[2] and Nabil A. Awadallah[1]
[1] Civil Engineering Dept., Faculty of Engineering, Fayoum University, Egypt
[2] Ministry of Water Resources and Irrigation, Egypt.

***Abstract*— Flash flooding can occur, even in hyper-arid regions, due to relatively short, intense burst of rainfall such as during a thunderstorm. Even though flash floods are localized, they present a significant hazard because of their unpredictability and commonly very short duration. To estimate peak discharges of flash floods, morphometric analysis is used to understand the nature of the hydrological processes in a basin, in order to develop a relationship that enables estimation of peak discharge values, in terms of morphometric parameters. The study is conducted using 28 flow gauging stations, in the northern region of Sultanate of Oman, in two steps. The first step is the extraction of morphometric parameters from available Digital Elevation Models. The second step is to develop relationships to estimate peak discharges, at different return periods, using linear and nonlinear regression methods. The best obtained relationship is a nonlinear one in terms of the total number of streams across all orders, the relative relief ratio, and the effective rainfall, with a coefficient of determination ranging from 0.979 to 0.997 and mean percentage absolute errors from 26% to 45%, for examined return periods.**

Keywords*— Flood, Morphometric Parameters, Peak discharge, Regression, Arid Region, Oman.

I. INTRODUCTION

Flash floods in arid regions have benefits and harms. The immediate impacts of flash flooding include loss of human life, damage to property, damage to power transmission and sometimes power generation, destruction of crops and loss of livestock. This triggered attention to many factors that affect floods such as topography, nature of the soil, and vegetated cover percentage to produce relationships to calculate the peak flow discharges at different return periods. Some of those relationships were expressed in terms of morphometric parameters, which result from the morphometric analysis of the drainage basins.

Several studies have explored the use of geomorphological characteristics. Developed relationships cover all climatic conditions. However, the current literature review focusses mainly on approaches to estimate flash floods and/or those developed in arid and semi-arid regions. Angillieri [1] studied the geomorphological characteristics of a basin with a stream order of 5 and a parallel dendritic pattern. The drainage density was found to be the parameter that affects floods patterns most. Bhatt and Ahmed [2] utilized GIS to extract the morphometric parameters to assess which of them influence flooding hazards the most. The main identified parameters include the ruggedness number (R_n) and the relief ratio (R_h), the stream frequency (F_s), the mean bifurcation ratio ($\bar{R}_b$), and the drainage density (D_d). Six large basins were selected in Saudi Arabia by Shi [3] to assess flood hazards. The morphometric basins parameters of the six basins and their related 203 sub-basins were combined to develop a relationship that predicts peak discharge values at different return periods provided.

In Oman, which is the study area of the current research, Al-Rawas [4] considered parameters like the drainage density, the relief ratio, the basin relief, the form factor, and the total basin area. He has also shown that it is possible to improve predictions of peak flow discharges by introducing other factors such as the extent of urbanization and the percentage of the vegetated cover area, which resulted in a significant improvement of peak discharges estimation, especially at high return periods. The developed equation was in terms of basin relief, relief ratio, total basin area, and the vegetated cover. The Ministry of Transport & Communications [5], Directorate of Roads and Land Transport, Sultanate of Oman, proposed an equation for northern Oman to predict the peak discharges at various return periods in terms of the catchment area, the slope of the maximum stream length within the basin, the estimated rainfall depth at the same return period, the runoff to rainfall ratio which was calculated based on the Soil Conservation Service SCS curve number model.

Morphometric analysis was also used for prioritization of sub-watersheds [6], extracting basin parameters using remote sensing [7,8,9,10,11], understand Paleo fluvial systems in the Kuwait [12], geo-hydrological studies [13], extract hydrologic indices [14], comparison between manual and automated delineation of basins [15], drainage basin asymmetry analysis [16], and many other applications.

The current research aims to investigate relationships between peak discharges and a large set of morphometric parameters, to identify the most influencing to be used in an arid region. Furthermore, to allow benefits in an operational context, these relationships have to produce accurate discharges and to show a robust behavior across return periods. The paper is organized as follows: After this introduction, the next two sections present the case study and the available data followed by the methodology. The results and discussion come next and finally the research conclusions and recommendations for future research.

International Journal of Engineering Research & Technology (IJERT)
ISSN: 2278-0181
Vol. 11 Issue 04, April-2022

II. CASE STUDY AND AVAILABLE DATA

The study focusses on the northern region facing the Arabian Gulf of Sultanate of Oman, which occupies the southeastern part of the Arabian Peninsula. The area of Oman is close to 309 500 $km2$ with most of it being an arid zone, subject to many flash floods that occurred in the years 1987, 1989, 1997, 2002, 2003, 2005, 2007, 2010, 2015 and 2020. The Mean Annual Rainfall (MAR) is 51 mm for the entire country, ranging from less than 20 mm in its deserts to over 350 mm in its rugged mountains. The study area consists of 10 basins monitored by 28 streamflow gauging stations (Figure 1).

The streamflow and rainfall frequency analysis results are obtained from the hydrology section report, issued by the Ministry of Transport and Communications [5], Directorate of roads and Land Transport, Oman, in the framework of the elaboration of the Highway Design Manual. Table S1 (in the supplementary material) summarizes the frequency analysis results of the flow gauging stations and the areal average of the daily rainfall depths at the same return periods.

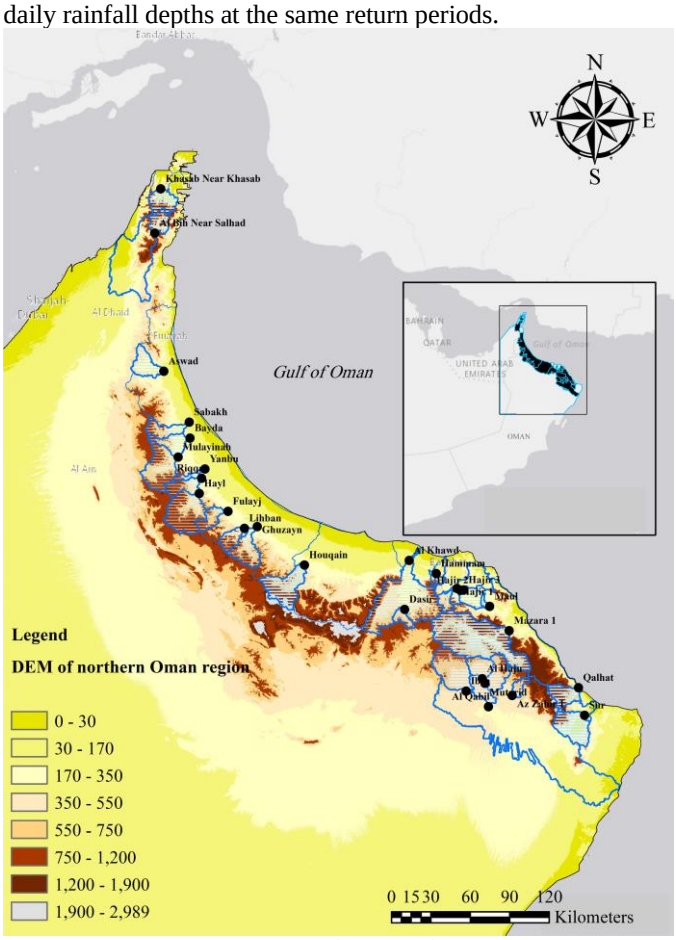

Fig. 1. Study area and location of available flow gauging stations.

III. METHODOLOGY

The methodology of this study consists of two stages: (i) Preparing input data through Basin's identification and preprocessing then the extraction of morphometric parameters from the digital elevation model (DEM) and through determining the effective rainfall; (ii) developing an equation to estimate the peak discharges at different return periods using linear and nonlinear regression analyses.

A. Basin's identification and preprocessing

Using 30-m DEM, whose source was the Shuttle Radar Topography Mission (SRTM) version 3 Plus [17], ten major basins are identified englobing all flow gauging stations. The extraction of the morphometric parameters of 28 drainage basins is created via ARC Hydro extension in ArcMap 10.4. These morphometric parameters are subdivided into four categories: drainage network, geometry, drainage texture, and basin relief parameters. Every category contains a group of parameters that describe the characteristics of the drainage basins.

B. Calculation of morphometric parameters

1) Drainage network parameters

In this category, the Stream Order (S), is determined based on the top-down Strahler method [18]. The Stream Number (N_s) defined as the number of streams in each order, the Total Numbers of Streams across all orders (TN_s), and the Stream Length (L_s), which is the total length of individual stream segments of each order, are also calculated [19]. Finally, the Bifurcation Ratio (R_b) is calculated, as per Equation (1) [20].

$$R_b = \frac{N_s}{N_{s+1}} \quad (1)$$

2) Geometry parameters

Geometry parameters include the areal and linear characteristics, such as the total surface area (A), the total basin perimeter (P), and the basin length (L_b), defined as the maximum dimension of the basin in the direction of the main drainage channel [21]. It encompasses also the form parameters that describe the shape of the basin, such as the Form Factor (F_f) [22], the Elongation Ratio (R_e) [21], defined by equations 2 and 3, respectively.

$$F_f = \frac{A}{{L_b}^2} \quad (2)$$

$$R_e = \frac{D_A}{L_b} \quad (3)$$

where D_A is the diameter of the circle with the same area as that of the basin.

3) Drainage texture parameters

These parameters include the Drainage density (D_d), defined as the ratio between the summation of all stream's length in a drainage basin to the area of the same drainage basin [23], the Stream frequency (F_s), which is the ratio between the number of streams in one basin to the basin area, and the Constant of channel maintenance (C), which is the inverse of the drainage density [21].

$$D_d = \frac{TL_s}{A_u} \quad (4)$$

$$F_s = \frac{TN_s}{A_u} \quad (5)$$

$$C = \frac{1}{D_d} \quad (6)$$

4) Basin relief parameters

These parameters include the Total Basin Relief (H), which is the difference between the maximum height of the basin and the height of the outlet for the same basin, the Relief Ratio (R_h), which is the ratio of the total basin relief to the basin length, the Relative Relief Ratio (R_p), which is the ratio between the total basin relief (H) and total basin perimeter (P)

International Journal of Engineering Research & Technology (IJERT)
ISSN: 2278-0181
Vol. 11 Issue 04, April-2022

[24], to finally obtain the value of the Ruggedness Number (R_n), which is the product of D_d by H [25].

$$R_h = \frac{H}{L_b} \quad (7)$$

$$R_p = \frac{H\ (feet)}{P\ (miles)} \quad (8)$$

$$R_n = D_d \times H \quad (9)$$

C. Calculating the effective rainfall depth

The effective rainfall, which is also used as a predictor of peak discharges, is calculated using the well-acknowledged Soil Conservation Service – Curve Number (SCS-CN) [26].

$$P_{eff}^{n} = \frac{(P_n - 0.2S_t)^2}{P_n + 0.8S_t} \quad (10)$$

Where P_{eff}^{n} is the effective rainfall depth (mm) corresponding to the rainfall depths at return period n, P_n is the rainfall depth (mm) at return period n, S_t is the potential storage of the soil (mm), which takes into account the CN, calculated as follows:

$$S_t = \left(\frac{1000}{CN} - 10\right) \times 25.4 \quad (11)$$

The CN relies on determining the hydrologic soil group and the land cover. Hydrologic Soil Groups are obtained from the Global Hydrologic Soil Groups (HYSOGs250m) dataset and hence the areal averages of the Curve Number for each basin are determined assuming a desert shrub cover of poor condition [27].

D. Developing relationships to estimate peak discharge using morphometric parameters

Relationships are developed to estimate peak discharges at various return periods equation. Linear and nonlinear regression equations are tested. The nonlinear equation is of the form:

$$Q_n = {X_1}^a \times {X_2}^b \times \ldots\ldots \times {X_i}^z \quad (12)$$

where:
Q_n is the peak discharge at return period n.
$X_1, X_2, \ldots, X_i$ are input variables.
$a, b, \ldots, z$ are the regression coefficients.

A stepwise regression method is used, via the Statistical Package for Social Sciences (SPSS) software [28], to select the most influential morphometric variables affecting the discharges. Beside the verification of the statistical significance of the regression coefficients to be included and the overall significance of the developed relationships, three performance criteria are calculated to assess the goodness of fit: R^2 (the adjusted coefficient of determination), the Mean Absolute Percentage Error ($MAPE$) and the Roof Mean Square Error ($RMSE$) defined as follows:

$$MAPE = 100 * \frac{1}{N} * \sum_{i=1}^{N} \frac{|y_i - \hat{y}_i|}{|y_i|} \quad (13)$$

$$RMSE = \sqrt{\frac{1}{N}\sum_{i=1}^{N}(y_i - \hat{y}_i)^2} \quad (14)$$

Where:
y_i, is the observed peak discharge;
$\hat{y}_i$ is the estimated peak discharge;
$\bar{y}_i$ is the average value for the observed series; and
N is the number of data points.

IV. RESULTS AND DISCUSSION

A. Morphometric characteristics of the 28 drainage basins

We present hereafter the major morphometric characteristics of the 28 drainage basins. Starting by the drainage networks characteristics, five basins are of second-order, twelve basins are of third-order, nine basins are of fourth order, and two basins area of fifth-order. On the other hand, the values of bifurcation ratios range between 2 and 7 and higher bifurcation ratio values are observed at lower stream orders in the mountains, while lower bifurcation ratio values are observed at higher stream orders where the area is characterized as flat. As for the average bifurcation ratio values, the maximum value is 6 for station No. 5, while the minimum value is 2.56 for station No. 1.

As for the geometrical and the drainage texture characteristics, two of the studied basins are circular, while the remaining basins are elongated with the possibility of low peak discharges. It is also found that the drainage densities are relatively low, ranging from 0.53 to 0.30, with an average value of 0.40. Investigating the stream frequencies, it is found that the frequency values are also low, where the maximum value is 0.10 and the minimum is 0.05 with an average value of 0.08. On the other hand, the constant channel maintenance values are high, which reflects strong control of lithology, where the range is between 3.36 and 1.89 with an average value of 2.55.

The drainage texture values are less than 2, which indicates that the surface of the basins is very coarse. As for the infiltration number values, they range from 0.05 to 0.02 with an average value of 0.03. The lengths of overland flow range from 1.68 km to 0.95 km. These high values indicate decreased values of drainage density and surface runoff with weak development of the drainage density.

For the relief characteristics, the maximum ruggedness number is 0.98 and the minimum number is 0.18 while the average is equal to 0.56, where these weak values express that the study region has weak dissection and erosion.

B. Developing relationships to estimate peak discharge

To develop an equation to estimate peak discharges at 2, 5, 10, 25, 50 and 100-year return periods, linear regression is first explored. The application of the linear regression with a constant term shows that the most influential variables are the area, the rainfall depths at the 100-year return period, the effective rainfall depths corresponding to the rainfall depths at the 100-year return period, and the total lengths of streams orders. By verifying the parameters' coefficients resulting from the linear regression analysis, it is noticed that the coefficient of the intercept is not statistically significant. Deleting the intercept term from the regression equation, the most influential parameters are the number of stream order 4, the length of stream order 1, the length of stream order 4, the total surface area, the rainfall depths at 100-year return period, and the effective rainfall depths corresponding to the rainfall depths at 100-year return period. The linear equation for the 100-year return period can be written as follows.

$$Q_{100} = 448.72N_{s4} - 0.015L_{s1} - 0.041L_{s4} + 5.43A - 8.14P_{100} + 14.95P_{eff}^{100} \quad (15)$$

where: Q_{100} is the peak discharge at 100-year return period, N_{s4} is the stream number of 4th stream order, L_{s1} is the length of streams of the 1st order, L_{s4} is the length of streams of the 4th

International Journal of Engineering Research & Technology (IJERT)
ISSN: 2278-0181
Vol. 11 Issue 04, April-2022

order, A is the Area, P_{100} is the rainfall depths at the 100-year return period and P_{eff}^{100} is the effective rainfall depths corresponding to the rainfall depths at the 100-year return period. This equation produces a $RMSE$ of 347.4 m^3/s, a $MAPE$ of 40.78% (which is rather high) with an adjusted R^2 of 0.95. Tables I to III provide the results of the analysis, while Figure 2 presents a plot of the predicted vs. the observed Q_{100}. Relationships for other return periods are also explored; however, for 2-year and 5-year return periods, no satisfactory equation, with statistically significant coefficients, is found.

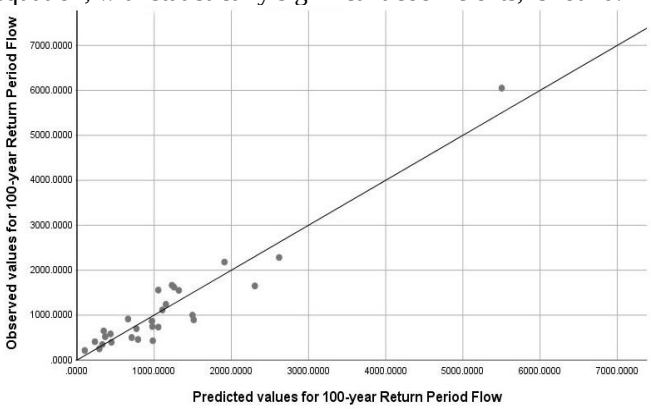

Fig. 2. Predicted vs. Observed Q_{100} using linear regression

TABLE I.

TABLE II. MODEL SUMMARY FOR LINEAR REGRESSION WITHOUT INTERCEPT TERM

Model	R	R^2	Adjusted R^2	Std-Error of the Estimate
6	0.975	0.951	0.938	391.7322402

TABLE III. ANOVA TABLE FOR SECOND SCENARIO LINEAR WITHOUT INTERCEPT TERM

Model		Sum of Squares	Df	Mean Square	F	Sig.
6	Regression	66144088.756	6	11024014.793	71.839	0.000
	Residual	3375991.257	22	153454.148		
	Total	69520080.013[d]	28			

TABLE IV.

COEFFICIENTS TABLE FOR LINEAR REGRESSION WITHOUT INTERCEPT TERM

Model		Unstandardized Coefficients		Standardized Coefficients	t	sig.
		B	Std. Error	Beta		
6	A	5.427	1.103	2.194	4.921	0.000
	P_{eff}^{100}	14.946	2.875	0.746	5.198	0.000
	P_{100}	-8.143	1.894	-0.694	-4.299	0.000
	L_{s4}	-0.041	0.012	-0.345	-3.333	0.003
	N_{s4}	448.721	168.938	0.222	2.656	0.014
	L_{s1}	-0.015	0.006	-1.125	-2.566	0.018

To obtain an improved relationship, the nonlinear option is explored and is transformed to the linear form using natural logarithms. The obtained relationship is described by equation 16.

$$\ln Q_{100} = 1.022 \ln TN_s + 0.594 \ln R_p + 0.868 \ln P_{eff}^{100} \quad (16)$$

where Q_{100} is the Peak discharge at the 100-year return period, TN_s is the total numbers of streams across all orders, R_p is the Relative Relief Ratio and P_{eff}^{100} is the effective rainfall depths corresponding to the rainfall depths at the 100-year return period.

The obtained relationship is simpler, yet it produces a lower $MAPE$ (compared to the linear equation with a larger number of variables) of 32.37% (calculated in the original scale of variables), a $RMSE$ of 335m^3/s, with an adjusted R^2 of 0.995. Tables IV to VI provide the full results of the analysis (calculated in the natural logarithm scale), while Figure 3 presents a plot of the predicted vs. the observed Q_{100}. Relationships for all return periods are also explored. All coefficients are found statistically significant.

TABLE V. MODEL SUMMARY FOR LINEAR REGRESSION OF NATURAL LOGARITHMS OF VARIABLES

Model	R	R^2	Adjusted R^2	Std-Error of the Estimate
1	0.996	0.995	0.994	0.4025221

TABLE VI. ANOVA TABLE FOR SECOND SCENARIO LINEAR REGRESSION OF NATURAL LOGARITHMS OF VARIABLES

Model		Sum of Squares	Df	Mean Square	F	Sig.
1	Regression	1279.617	3	426.539	2632.565609	0.000
	Residual	4.051	25	0.162		
	Total	1283.667	28			

TABLE VII. COEFFICIENTS TABLE FOR LINEAR REGRESSION OF NATURAL LOGARITHMS OF VARIABLES

Model		Unstandardized Coefficients		Standardized Coefficients	t	sig.
		B	Std. Error	Beta		
6	$\ln TN_s$	1.022	0.081	0.485	12.593	0.000
	$\ln R_p$	0.594	0.201	0.40	2.960	0.007
	$\ln P_{eff}^{100}$	0.868	0.063	0.530	13.839	0.000

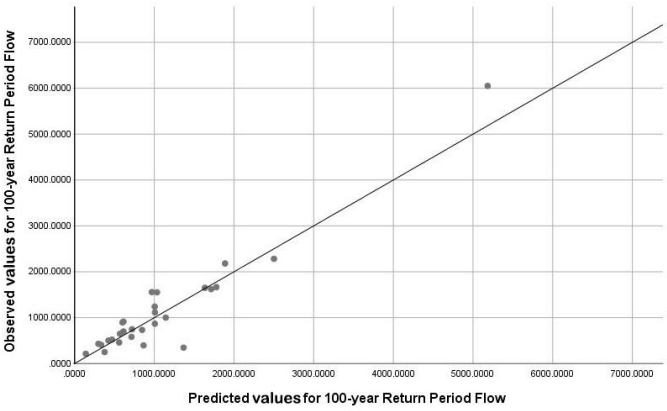

Fig. 3. Predicted vs. Observed Q_{100} using nonlinear regression

International Journal of Engineering Research & Technology (IJERT)
ISSN: 2278-0181
Vol. 11 Issue 04, April-2022

By applying the same nonlinear form, for of streams of the 50-, 25-, 10-, 5-, and 2-year return periods, the following equations (17 to 21) are obtained:

$$\ln Q_{50} = 1.046 \ln TN_s + 0.581 \ln R_p + 0.852 \ln P_{eff}^{50} \quad (17)$$

$$\ln Q_{25} = 1.1 \ln TN_s + 0.603 \ln R_p + 0.809 \ln P_{eff}^{25} \quad (18)$$

$$\ln Q_{10} = 1.247 \ln TN_s + 0.733 \ln R_p + 0.662 \ln P_{eff}^{10} \quad (19)$$

$$\ln Q_5 = 1.419 \ln TN_s + 0.931 \ln R_p + 0.414 \ln P_{eff}^{5} \quad (20)$$

$$\ln Q_2 = 1.409 \ln TN_s + 0.837 \ln R_p + 0.128 \ln P_{eff}^{2} \quad (21)$$

The $MAPE$ for Q_{50}, Q_{25}, Q_{10}, Q_5 and Q_2 are 26.1%, 27.83%, 37.31%, 44.44% and 45.13%, respectively with adjusted R^2 of 0.997, 0.996, 0.993, 0.986 and 0.979, respectively. Figures 4 and 5 show plots between the relative errors for various return periods and the total No. of streams across all orders and the relative relief ratio values.

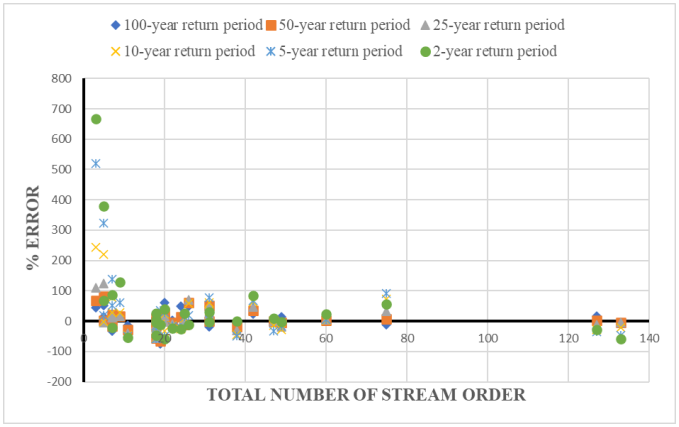

Fig. 4. Relative errors for various return periods vs. TN_s

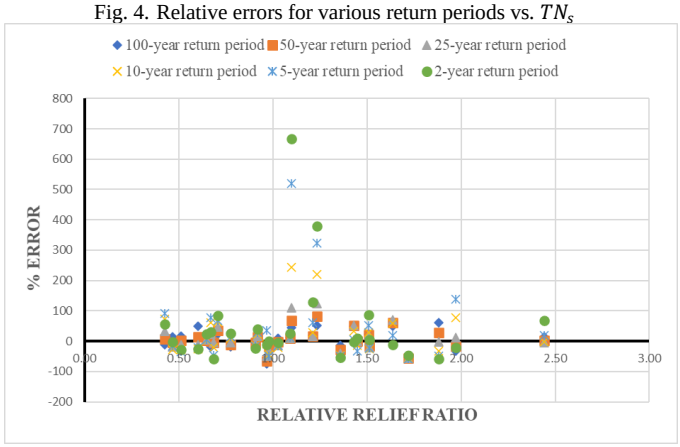

Fig. 5. Relative errors for various return periods vs. R_p

V. Conclusions and Recommendations

The aim of this research is to develop relationships that estimate peak flow discharge at various return periods. The study area is located in the northern region of the Sultanate of Oman, which consists of 10 basins monitored by 28 peak flow discharges stations. Morphometric parameters are extracted and analyzed to shed light on the basins underlying hydrologic processes and their eventual response to floods.

Using a stepwise regression approach, linear and nonlinear relationships are developed between selected morphometric parameters and peak discharges at various return periods. A linear equation is developed in terms of the length of streams for order 4, the number of streams for order 4, the length of streams for order 1, the area, the rainfall depths at 100-year return period, and the effective rainfall depths corresponding to the rainfall depths at 100-year return period. As for the nonlinear regression analysis, the developed relationship is in terms of the total numbers of stream across all orders, the relative relief ratio, and the effective rainfall depths corresponding to the rainfall depths at the 100-year return period. The linear equation produces a $MAPE$ of 40.78% with an adjusted R^2 of 0.95 but the nonlinear equation (which has a fewer number of input variables) shows better performance and produces a $MAPE$ of 32.37% with an adjusted R^2 of 0.995.

Recommendations for future research include to extend the study to more gauged basins in arid regions, to relate the morphological parameters to the time of concentration of the basins calculated via calibration of the observed flows, and to extend the study to produce relationships to estimate average runoff values and not only peak discharges.

References

[1] M. Y. E. Angillieri, “Morphometric analysis of Colangüil river basin and flash flood hazard, San Juan, Argentina,” 1st ed., vol. 55. Environmental Geology, 2008, pp. 107-111.

[2] S. Bhatt, and S. A. Ahmed, “Morphometric analysis to determine floods in the Upper Krishna basin using Cartosat DEM,” 8th ed., vol. 29. Geocarto international, 2014, pp. 878-894.

[3] Q. Shi, “Flood hazard assessment along the Western Regions of Saudi Arabia using GIS-based morphometry and remote sensing techniques,” MSc Thesis, King Abdullah University of Science and Technology, Thuwal, Kingdom of Saudi Arabia, 2014.

[4] G. A. A. Al-Rawas, “Flash flood modeling in Oman wadis,” OhD Thesis, Department of Civil Engineering, University of Calgary, 2009.

[5] Highway design manual of Oman hydrology section, Directorate of Roads and Land Transport, Ministry of Transport and Communications, Sultanate of Oman, 2010.

[6] S. Biswas, S. Sudhakar, and V. R. Desai, “Prioritization of subwatersheds based on morphometric analysis of drainage basin: A remote sensing and GIS approach,” 3rd ed., vol. 27. Journal of the Indian society of remote sensing,1999, pp. 155-166.

[7] R. Chopra, R.D. Dhiman, and P.K. Sharma, “Morphometric analysis of sub-watersheds in Gurdaspur district, Punjab using remote sensing and GIS techniques,” 4th ed., vol. 33. Journal of the Indian Society of Remote Sensing, 2005, pp. 531-539.

[8] M. Kamala, and M. Samynathan, “Morphometric Analysis of Drainage Basin Using GIS Techniques: A Case Study of Amaravathi River Basin, Tamilnadu,” 7th(F) ed., vol. 9. International Journal of Recent Scientific Research, 2018, pp. 28142-28147.

[9] D. Mishra, B. N. Singh, and D. K. Behera, “Morphometric Analysis of Bara Tehsil of Allahabad District Through Cartosat-1 DEM Data,” 1st ed., vol. 6. International Journal of Creative Research Thoughts (IJCRT), 2018, pp. 1897-1907.

[10] P. D. Sreedevi, S. H. H. K. Owais, H. H. Khan, and S. Ahmed, “Morphometric analysis of a watershed of South India using SRTM data and GIS,” 4th ed., vol. 73. Journal of the geological society of India, 2009, pp. 543-552.

[11] S. S. Vittala, S. Govindaiah, and H. H. Gowda, “Morphometric analysis of sub-watersheds in the Pavagada area of Tumkur district, South India using remote sensing and GIS techniques,” 4th ed., vol. 32. Journal of the Indian Society of Remote Sensing, 2004, pp. 351-362.

[12] R. Mohammad, “Geographical Information System Based Analysis of Paleo fluvial Systems in the Kuwait Region,” MSc Thesis, Department of Geology, School of Arts and Sciences, University of Pittsburgh, 2008.

[13] R. A. Hajam, A. Hamid, and S. Bhat, “Application of morphometric analysis for geo-hydrological studies using geo-spatial technology–a case study of Vishav Drainage Basin,” 3rd ed., vol.4. Hydrology Current Research, 2003, pp. 1-12.

[14] S. Karalis, et al. “Assessment of the relationships among catchments’ morphometric parameters and hydrologic indices,” 5th ed., vol.13. International Journal of Geosciences, 2014, pp. 1571.

International Journal of Engineering Research & Technology (IJERT)
ISSN: 2278-0181
Vol. 11 Issue 04, April-2022

[15] M. Y. E. Angillieri, and O. M. Fernández, "Morphometric analysis of river basins using GIS and remote sensing of an Andean section of Route 150, Argentina. A comparison between manual and automated delineation of basins," 2nd ed., vol. 34. Revista mexicana de ciencias geológicas, 2017, pp. 150-156.
[16] D. Baioni, (2016). "Analysis of Drainage Basin Asymmetry in the Ventana River, Northern Apennines (Central Italy)", 1st ed., vol.121. International Journal of Earth & Environmental Sciences, 2016, pp. 1-5.
[17] NASA, Shuttle Radar Topography Mission (SRTM) version 3 Plus, Void free dataset, https://lpdaac.usgs.gov/products/srtmimgrv003/, 2015.
[18] A.H. Strahler, "Dynamic Basis of Geomorphology," vol. 63. Geological Society of America Bulletin, 1952, pp. 923-938.
[19] K.G. Smith, (1950). "Standards for grading texture of erosional topography," 9th ed., vol.248. American Journal of Science, 1950, pp. 655-668.
[20] A.H. Strahler, "Quantitative Geomorphology of Drainage Basins and Channel Networks," In: Chow, V., Ed., Handbook of Applied Hydrology, McGraw Hill, New York, pp. 439-476, 1964.
[21] S.A. Schumm, "Evolution of drainage systems and slopes in badlands at Perth Amboy", 5th ed., vol. 67. Geological Society of America Bulletin. New Jersey, 1956, pp. 597-646.
[22] R.E. Horton, "Drainage-basin characteristics", Eos Trans. AGU, vol. 13, pp. 350-361, 1932.
[23] R.E. Horton, "Erosional development of streams and their drainage basins: Hydrophysical approach to quantitative morphology", Geol. Soc. Amer. Bull., vol. 56, pp. 275-360, 1945.
[24] M.A. Melton, "An analysis of the relations among elements of climate, surface properties, and geomorphology", Columbia University, New York, 1957.
[25] A.H. Strahler, and A. Strahler, "Introducing physical geography", New York: Wiley, 2013.
[26] USDA (United States Department of Agriculture), Urban hydrology for small watersheds, Technical release, no 55 (TR-55). Soil Conservation Service (SCS), Washington, DC, 1986.
[27] C.W. Ross, et al. "Global Hydrologic Soil Groups for Curve Number-Based Runoff Modeling (HYSOGs250m)", ORNL DAAC, Oak Ridge, Tennessee, USA. https://doi.org/10.3334/ORNLDAAC/1566, 2018.
[28] IBM Statistical Package for Social Sciences, last accessed, https://www.ibm.com/products/spss-statistics, April 2022.

International Journal of Engineering Research & Technology (IJERT)
ISSN: 2278-0181
Vol. 11 Issue 04, April-2022

TABLE S1. FREQUENCY ANALYSIS RESULTS OF THE STREAMFLOW AT THE GAUGING STATIONS IN NORTH OMAN

	Return Periods (years) Return Periods (years)											
	2	5	10	25	50	100	2	5	10	25	50	100
Station ID	**Rainfall (mm)**						**Flow (m^3/sec)**					
Al Haju	25.5266	45.9267	61.7977	85.6321	106.8273	131.7804	63.1	149.3	223.1	340.9	450.3	581.9
Al Khawd	28.0086	45.0199	57.8313	77.3542	95.7721	119.5013	182.2	458.7	722.2	1,187.20	1,662.40	2,282.90
Al Qabil	25.5543	45.3459	60.4363	82.5873	102.0995	125.0799	257.1	466.9	601.3	766.2	885.1	1,000.30
Aswad	29.0159	51.4752	68.2597	92.1047	111.9861	133.8655	56.9	170.2	305.8	602.8	974.3	1,552.20
Az-Zahir 1	27.3975	45.6224	58.2137	74.7786	88.8173	105.6090	49.2	105.9	155.6	236.9	314	408.6
Bayda	28.9517	49.0594	64.3791	86.5181	105.2802	126.1991	53.9	136.7	218.9	369.9	530.3	746.6
Dasir	28.0344	44.0919	55.5522	71.8504	86.0520	102.9803	77.5	147.7	207.9	304.2	393.8	501.7
Fulayj	29.5455	48.7032	63.4086	85.3456	104.9945	128.3451	75.7	191.6	310.2	534.4	778.5	1,115.20
Ghuzayn	25.8687	42.4364	55.2441	74.2861	91.1553	110.8873	118.3	291.9	469.2	803.1	1,166.00	1,665.60
Hajir 1	22.2801	42.4666	59.6023	87.5287	114.5510	148.8266	21.6	69.2	128.9	265.9	444.7	733.2
Hajir 2	19.1242	39.0019	56.8761	87.3439	117.9233	157.6807	21.1	54.5	84.8	136.1	186.5	250.1
Hajir 3	21.0202	47.6535	74.0773	123.2076	176.4796	250.1670	50.55	112.18	159.26	226.99	283.96	346.88
Hammam	22.9344	44.2485	62.2564	91.5553	120.1050	156.7727	44.8	101.8	166.4	300.6	460.4	698.5
Hayl	28.7206	46.5384	59.6603	78.4386	94.4864	112.7616	300.6	578.8	792.3	1100.9	1361.5	1650.4
Houqain	31.9282	47.8533	58.1182	70.8629	80.1957	89.3757	145.91	326.14	453.22	623.19	756.45	895.08
Ibra	43.7961	67.5225	83.3288	103.9365	119.9982	136.8623	184.21	464.112	723.35	1169.03	1613.32	2181.05
Lihban	27.8773	42.6513	53.8911	70.6816	86.0750	104.8581	112.8	228.5	331.3	501.5	665.1	867.8
Maul	21.9370	46.8962	70.5411	113.0987	158.1655	219.5834	47.4	114.6	170.6	257.9	337.2	430.7
Mazara 1	25.4710	45.5658	61.3427	85.5396	107.7388	134.7869	483.6	1,192.90	1,878.50	3,104.90	4,374.40	6,050.10
Mulayinah	28.0036	46.5979	60.6756	80.9737	98.1891	117.4469	234.9	461.4	627	856.2	1,041.80	1,240.30
Mutarid	25.3417	44.5111	58.8649	79.7141	98.0799	119.8371	91.2	179.7	242.1	325.7	391.1	459.3
Qalhat	22.6451	37.3307	47.3589	60.3282	71.0200	83.4860	60.5	191.9	340.4	647.9	1,013.40	1,556.90
Riqqah	28.2156	45.8042	58.5863	76.4321	91.1606	107.2898	69.6	133.6	192.7	293.7	394.1	521.8
Sabakh	28.2540	48.0942	62.8274	83.6653	100.9762	119.9733	77.9	164.1	241.3	369.8	494.1	648.9
Sur	25.4959	44.8019	59.7473	79.8306	98.8334	125.1173	150.9	341.5	524.4	849.2	1,183.10	1,621.40
Yanbu	27.7224	45.4225	58.4640	76.8554	92.1386	108.9188	47.5	91.8	121.1	158.4	186.1	213.6
Al Bih Near Salhad	45.7548	74.2834	92.6443	116.1033	134.1467	152.9760	52.1	112.6	162.9	241.3	312.4	396.2
Khasab Near Khasab	27.8773	42.6513	53.8911	70.6816	86.0750	104.8581	81.8	191.9	296.5	480.9	668.9	913.9